RESOURCE GEOLOGY, vol. 56, no. 1, 49–54, 2006

Short Communication

A Possible Role of Boiling in Ore Deposition: A Numerical Approach

Kenichi HOSHINO, Toru ITAMI[1], Ryouta SHIOKAWA and Makoto WATANABE

Department of Earth and Planetary Sciences, Hiroshima University, Higashi-Hiroshima 739-8526, Japan [hoshino@geol.sci.hiroshima-u.ac.jp]

[1] *Present address: NextCom, 3-26 Kanda-Nishikicho, Chiyoda-ku, Tokyo 101-0054, Japan*

Received on April 28, 2005; accepted on October 1, 2005

Abstract: A possible role of boiling of the H_2O-NaCl-CO_2(-H_2S) fluid in ore deposition has been examined numerically by using the equations of state (EOS) of Duan et al. (1995, 1996), a modified EOS of Bowers and Helgeson (1983) and the water-rock interaction simulator MIX99 (Hoshino et al., 2000).

The following three models are examined to evaluate an efficiency of boiling on mineral precipitation: (1) hypothetical non-boiling process, (2) hypothetical boiling process with sulfur partitioned only in liquid phases and (3) boiling process in which partition ratios of H_2S between liquid and vapor phases are assumed to be the same as those of CO_2. The processes are simulated from 450°C and 900 bar to 310°C and 620 bar with an analytical step of 10°C / 20 bar. Boiling occurs below 400°C in the latter two processes when the initial composition (in mole fraction) of the fluid is: $X_{H_2O} = 0.84$, $X_{NaCl} = 0.10$ and $X_{CO_2} = 0.06$.

Ore deposition occurs abruptly at a boiling point when the partition ratios of total sulfur (X_s^{vap}/X_s^{liq}) are as high as those of total carbon during boiling. A decrease of concentration of sulfur in the liquid phase during boiling leads to an increase of pH of the solution, resulting in propelling mineral precipitation. It has been made clear that a possible role of boiling in ore formation mainly depends on the partition ratios of sulfur between the liquid and vapor phases, although they cannot be estimated accurately by the currently available EOS.

Keywords: boiling, ore deposition, equation of state (EOS), water-rock interaction, simulation

1. Introduction

It has been often proposed that boiling of ascending fluids may be a direct cause of ore deposition (e.g., Kamilli and Ohmoto, 1977; Lyakhov and Popivnyak, 1978; Robert and Kelly, 1987; Bottrell et al., 1988; Naden and Shepherd, 1989 and Wilkinson and Johnston, 1996). Mineralization caused by the onset of immiscibility of H_2O-CO_2 fluids has been theoretically analyzed to evaluate the role of boiling in mineral precipitation (e.g., Drummond and Ohmoto 1985; Cole and Drummond, 1986 and Bowers, 1991). Akinfiyev (1995) also theoretically analyzed galena precipitation from boiling fluids of the H_2O-CO_2-NaCl-H_2S system. Those analyses were based on the phase relation of the H_2O-CO_2 system, and hence only for low temperature conditions (< 350°C).

A recent development of the equation of state (EOS) has made it possible to predict phase equilibria for the H_2O-NaCl-CO_2 system at high P-T conditions. Therefore, we have numerically simulated ore deposition associated with boiling of the H_2O-NaCl-CO_2 solvent by using EOS in order to evaluate the possible role of high-temperature boiling in ore formation.

2. Analyzed Condition

A general image of an ore-formation process associated with boiling is shown in Figure 1. An ore-forming fluid of high temperature and high metal concentrations is formed probably by mixing of circulating meteoric water and magmatic fluid (Hoshino et al., 2000). With ascent of the fluid, it boils due to a decrease in pressure, resulting in a change of the fluid composition. If such compositional change is effective for mineral precipitation, fluid boiling could be responsible for the formation of ore deposits.

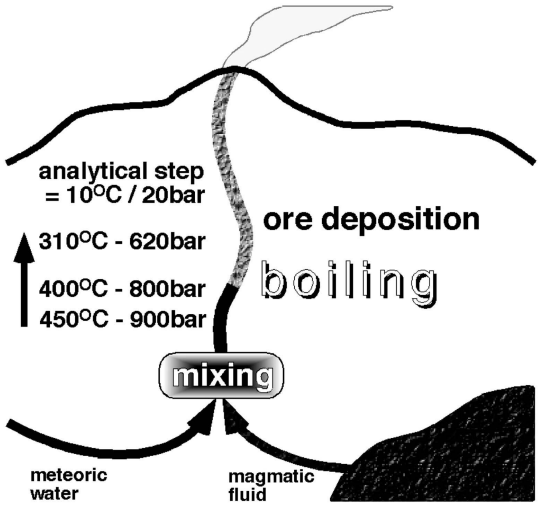

Fig. 1 An analyzed model for ore deposition with boiling. Ascending fluids are simulated from P = 900 bar and T = 450°C to P = 620 bar and T = 310°C with an analytical step of 10°C / 20 bar.

2.1. Equations used for model analysis

Many investigations of fluid inclusions present in ore deposits revealed that ore-forming fluids can be approximated by the H_2O-NaCl-CO_2 system (e.g., Wilkinson and Johnston, 1996). Although EOS by Bowers and Helgeson (1983; BH EOS hereafter) for this system is well known, it cannot predict phase equilibria (Fig. 2). On the other hand, EOS proposed by Duan et al. (1995; DMW95 EOS) can be used to draw the phase diagram for the system above 300°C (Fig. 2). Hence, we have used the latter EOS for calculation of the solvent composition of boiling fluids in the present analysis.

Since the ore-forming fluid may ascend rapidly, it is quite possible that boiling of the fluid is an isenthalpic or semi-isenthalpic process. Enthalpy of the solvent of the H_2O-NaCl-CO_2 system can be calculated by the following equations:

$$H = H^{id} + H^{ex}, \quad (1)$$

where ideal gas enthalpy H^{id} is

$$H^{id} = \Sigma_{x_i} \cdot H_i^{id}, \quad (2)$$

and excess enthalpy H^{ex} of the mixture is

$$H^{ex} = -RT^2 \Sigma xi \cdot \left(\frac{\partial \ln \phi_i}{\partial T}\right)_p, \quad (3)$$

where R, T, xi and ϕ_i are the gas constant, temperature in K, mole fraction and fugacity coefficient of i in the mixture, respectively, and also by the equation as

$$H = H^{id} - \Delta H', \quad (4)$$

where residual enthalpy ΔH' is

$$\Delta H' = -RT(Z-1) - RT^2 \int_{-\infty}^{v} \frac{1}{V} \left(\frac{\partial Z}{\partial T}\right)_v dV, \quad (5)$$

where V and Z represent volume and compressibility factor of the mixture, respectively.

Since BH EOS is the modified Redlich-Kwong type, we can obtain analytical solutions for Equations 3 and 5. On the other hand, the derivative in Equation 3 is obtained numerically for DMW95 EOS because of its complication. Calculated enthalpies are shown in Figure 3. Both EOS's give physically unlikely enthalpy profiles for the H_2O-NaCl solutions. If the enthalpy of the homogeneous fluid increases with decreasing temperatures as shown in the figure, the fluid may need heat for cooling. The results mean that the EOS's are not sufficiently accurate for enthalpy calculations. Therefore, we cannot simulate the process of isenthalpic boiling of the H_2O-NaCl-CO_2 fluid. Hence, we have analyzed the model in which the fluid is thermally equilibrated with surrounding rocks, that is, the temperature and pressure of the fluid are externally controlled.

Although H_2S, a dominant dissolved species of sulfur

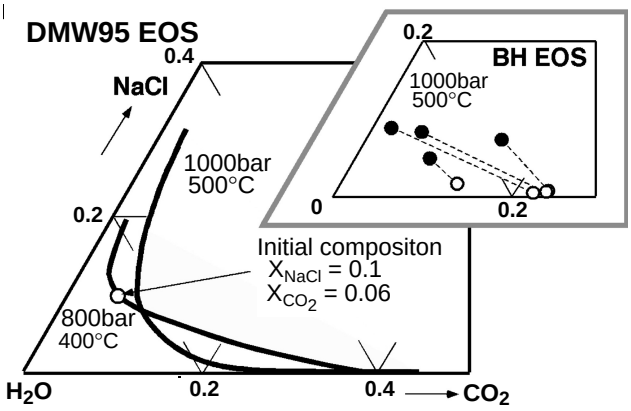

Fig. 2 Phase analyses for the H_2O-NaCl-CO_2 system at P = 1000 bar and T = 500°C (DMW95 EOS and BH EOS) and P = 800 bar and T = 400°C (DMW95 EOS). Solid and open circles in the inset represent compositions of liquid and vapor phases, respectively.

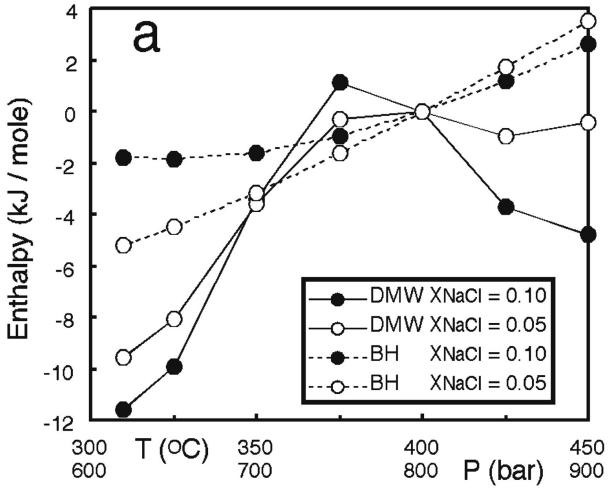

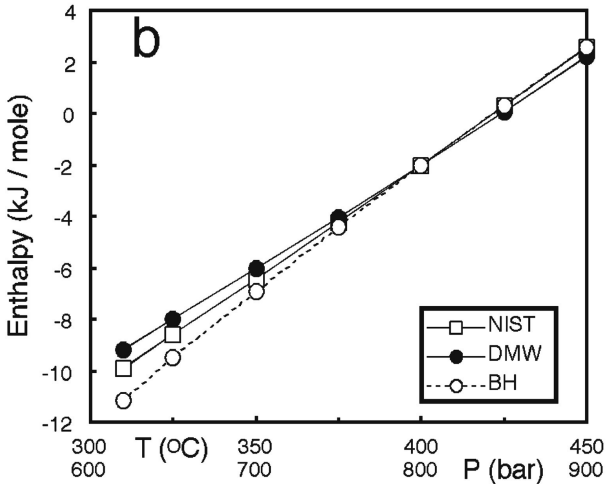

Fig. 3 Enthalpy analyses for H_2O-NaCl solution (a) and pure H_2O (b). Enthalpies are normalized as H = 0 at P = 800 bar and T = 400°C. NIST data (Chase, 1998) for pure H_2O are also plotted.

in the present analysis, is probably partitioned into vapor (low density) phases during boiling, no EOS for the H_2O-NaCl-CO_2-H_2S system has so far been proposed. Although the dielectric constants of fluids with high NaCl and CO_2 contents have been tried to estimate (e.g., Xie and Walther, 1995; Akinfiyev, 1995 and Wang and Anderko, 2001), a reliable equation to calculate the constants for the H_2O-NaCl-CO_2 fluid at high temperatures has not been developed. Therefore, we cannot accurately calculate the partition of H_2S between the liquid (high density) and vapor phases based on their fugacity coefficients. However, we may approximately suppose the partition from EOS of Duan et al. (1996; DMW96 EOS) for the H_2O-CO_2-H_2S system and BH EOS by the following way. Firstly, a volume of pure H_2S at an interesting P-T condition is calculated by DMW96 EOS. Then the volume is substituted in BH EOS to obtain a-parameter of BH EOS for H_2S. Its b-parameter can be taken from Holloway (1981). By assuming that those parameters are not affected by the presence of salts (Bakker, 1999), we can now approximately analyze phase equilibrium for the H_2O-NaCl-CO_2-H_2S system by the modified BH EOS at a specified P-T condition. A representative phase analysis for the system calculated in this way is presented in Table 1, as well as that for the H_2O-NaCl-CO_2 system obtained by DMW95 EOS. It is clear that H_2S is strongly partitioned into the gas phase like CO_2. Because BH EOS and hence the modified EOS are not accurate and can predict phase equilibria only for a limited condition as stated above, we may assume that the partition ratios of total sulfur (S) is the same as that of total carbon (C) if their major dissolved species are H_2S and CO_2, respectively. Since we cannot calculate the accurate dielectric constants of the solvent up to now, an additional assumption is made that solutes other than H_2S remain in liquid phases during boiling.

MIX99 (Hoshino et al., 2000) combined with the data set of SUPCRT92 (Johnson et al., 1992) is used for the present analysis. Hence, the dielectric constants of the solvent are implicitly taken as those of pure water calculated in SUPCRT92 for given P-T conditions. The constants are also used in the equations for calculating activity coefficients of solutes given by Helgeson and Kirkham (1976).

2.2. Initial condition

The initial fluid composition is (in mole fraction): X_{H_2O} = 0.84, X_{NaCl} = 0.10 and X_{CO_2} = 0.06, which is homogeneous at the condition of 400°C and 800 bar, and will boil slightly below the condition. Elements dissolved in the solvent are Fe, Cu, Zn, Pb, K, Si, Ca and S. The initial pH and logf_{O_2} at 400°C and 900 bar are 6.0 and –30, respectively. Concentrations of K, Si and S are taken from seawater data. Metal element concentrations are set as slightly below the solubilities of respective ore minerals at the conditions. Total charge of the initial fluid is balanced by

Table 1 Phase analyses for the H_2O-NaCl-CO_2(-H_2S) system at P = 780 bar and T = 390°C by BH EOS modified in the present study (a) and DMW95 EOS (b).

(a)

X(gas) =0.4057	Initial	Liquid phase		Gas phase	
	X	X	ϕ	X	ϕ
H_2O	8.396E-1	8.445E-1	2.793E-1	8.324E-1	2.834E-1
NaCl	1.000E-1	1.431E-1	1.959E-1	3.692E-2	7.588E-1
CO_2	6.000E-2	1.222E-2	4.240E+1	1.300E-1	3.985E+0
H_2S	4.000E-4	2.272E-4	5.795E+0	6.531E-4	2.016E+0

(b)

X(gas) =0.0268	Initial	Liquid phase		Gas phase	
	X	X	ϕ	X	ϕ
H_2O	8.400E-1	8.465E-1	2.524E-1	6.059E-1	3.527E-1
NaCl	1.000E-1	1.027E-1	1.239E-7	1.217E-3	1.046E-5
CO_2	6.000E-2	5.082E-2	1.116E+1	3.929E-1	1.444E+0

X: mole fraction; ϕ: fugacity coefficient

Table 2 Initial conditions and dissolved species encountered in the present analysis.

P = 800bar, T = 400°C, pH = 6.0, Log f_{O_2} = -30
X(H_2O) = 0.84, X(NaCl) = 0.10, X(CO_2) = 0.06

Element	Dissolved species	Total
Na	Na^+, NaCl, $NaSO_4^-$, $NaHSiO_3$	
Cl	Cl^-, NaCl, KCl, $FeCl^+$, $FeCl_2$, $CuCl_2$, $CuCl_2^-$, $ZnCl^+$, $ZnCl_2$, $ZnCl_3^-$, $PbCl^+$, $PbCl_2$, $PbCl_3^-$, $CaCl^+$, $CaCl_2$	
C	HCO_3^-, CO_2, CO_3^{--}, $Ca(HCO_3^-)^+$, $CaCO_3$	
K	K^+, KCl, KSO_4^-	1.020E-2
Si	SiO_2, $HSiO_3^-$, $NaHSiO_3$	7.120E-5
S	SO_4^{--}, HSO_4^-, H_2S, HS^-, $NaSO_4^-$, KSO_4^-, $CaSO_4$	2.820E-2
Fe	Fe^{++}, $FeCl^+$, $FeCl_2$	3.000E-5
Cu	Cu^{++}, $CuOH^+$, $CuCl_2$, Cu^+, $CuCl_2^-$	4.000E-6
Zn	Zn^{++}, $ZnOH^+$, $ZnCl^+$, $ZnCl_2$, $ZnCl_3^-$	2.000E-5
Pb	Pb^{++}, $PbCl^+$, $PbCl_2$, $PbCl_3^-$	1.000E-5
Ca	Ca^{++}, $CaCl^+$, $CaCl_2$, $Ca(HCO_3^-)^+$, $CaCO_3$, $CaSO_4$	1.711E-3

Total = total concentrations in mole/kg-water

total Ca = 1.71×10^{-3} (mol/kg-water). All dissolved species counted in the present analysis other than H^+, OH^-, $H_{2,aq}$ and $O_{2,aq}$ are listed in Table 2. Simulated minerals are quartz, calcite, anhydrite, hematite, magnetite, pyrite, pyrrhotite, chalcopyrite, bornite, sphalerite and galena.

The initial fluid is heated up to 450°C and 900 bar without mineral reactions. Then, ore-formation processes with and without boiling are analyzed from T = 450°C and P = 900 bar to T = 310°C and P = 620 bar with an analytical step of 10°C / 20 bar. The fluid with the above composition begins to boil below 400°C according to DMW95 EOS. A vapor phase is removed from the system in each analytical step.

Note that precipitated minerals are assumed not to reract with the solution in each analysis, because we analyze the first solution which percolates through individual

T-P points only at once. A temporal change in a mineral assemblage caused by continuously percolating fluid is another problem.

3. Results

The following three models are analyzed in order to evaluate a possible role of boiling in mineral precipitation and to examine an essential factor to control the role:

1) process without boiling,

2) process with boiling during which S remains in a liquid phase, and

3) process with boiling with assumed same partition ratios of S and C.

Although the processes 1) and 2) are unrealistic in nature, they may be worth being analyzed for the evaluation of the role by comparing the analytical results among the three models.

3.1. Process without boiling

The analytical results of the process without boiling are shown in Figure 4-a. Major dissolved species of C and S are CO_2 and H_2S, respectively, throughout the process. As is evident, a gradual decrease of pH of the cooling fluid restrains mineral deposition in this model. However, a decrease in solubilities of sulfide minerals with decreasing temperatures leads to precipitation of chalcopyrite and pyrite below 370°C.

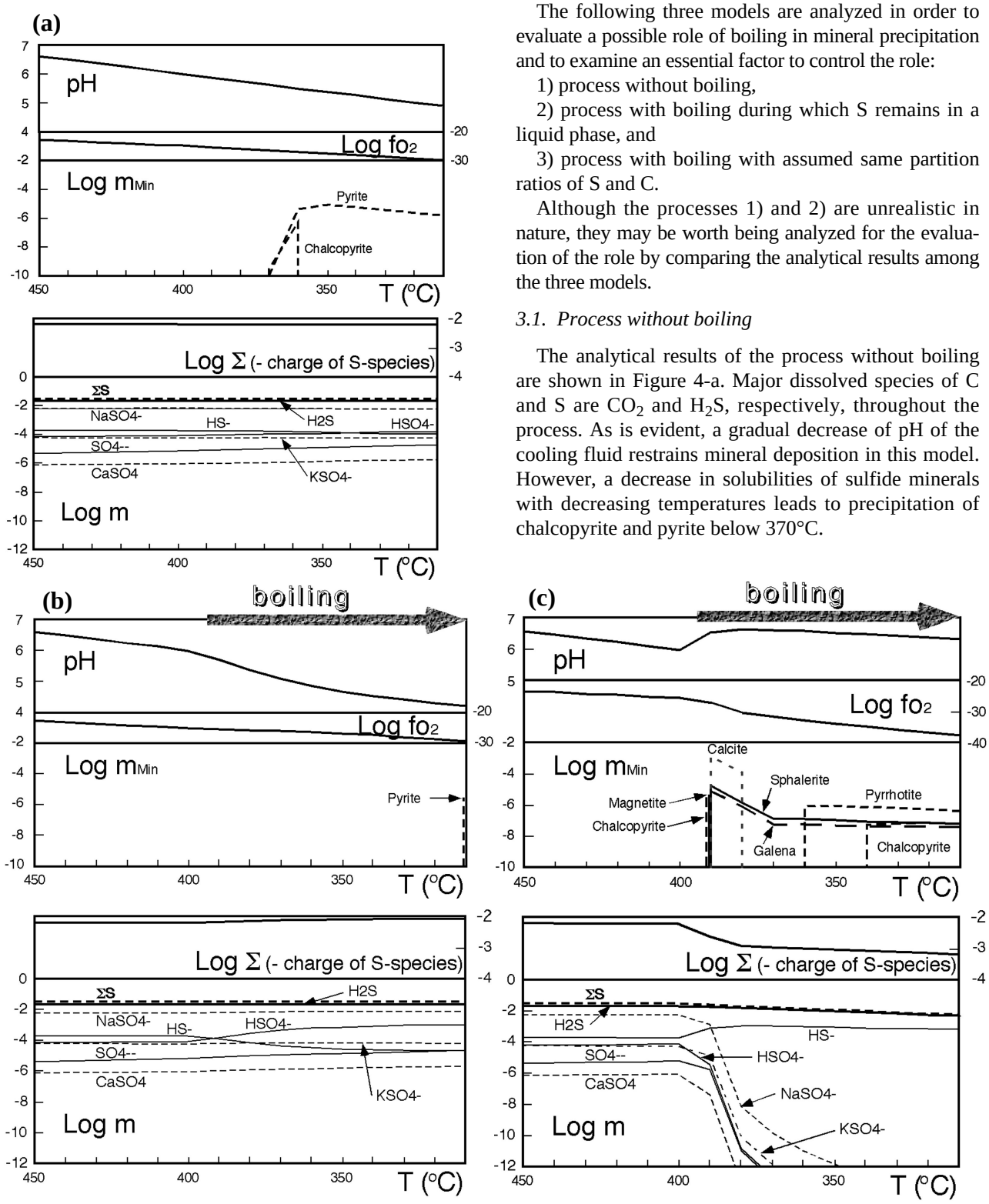

Fig. 4 Simulation results: (a) process without boiling, (b) process with boiling during which S remains in a liquid phase and (c) process with boiling with assumed same partition ratios of S and C. Mineral precipitation and concentrations of dissolved species are plotted by mole/kg-water.

3.2. *Process with boiling during which S remains in a liquid phase*

The fluid with the initial compositions begins to boil below 400°C in this model (Fig. 4-b). The degassing ratios (X_{vap}) for one analytical step (10°C / 20 bar) decrease from 0.0268 at 400–390°C to 0.0032 at 320–310°C. A totally degassed amount from the fluid throughout the analyzed process is only about 11 % of the initial amount. Therefore, degassing associated with continuous boiling will bring only minor increase in the dissolved elements in the liquid phase. Major dissolved species of C and S throughout the process are also CO_2 and H_2S, respectively. The partition ratios of C (X_C^{vap}/X_C^{liq}) is 7.73 at the first boiling step (400–390°C). Because of the small degassing ratio, the decrease of C concentration in the liquid phase during the step is small (from 0.06 to 0.0508). It is interesting to note that the decrease of pH of the liquid phase becomes much larger than the previous model. This may be due to an increase of $NaSO_4^-$, the second major dissolved species of S, during boiling. As a result, only pyrite precipitates at the final analytical step.

3.3. *Process with boiling with assumed same partition ratios of S and C*

The analytical results of this model are shown in Figure 4-c. Although the decrease of C concentration in the liquid phase during the first boiling step is as small as in the second model, a concomitant decrease of S at the step leads to an increase in the solution pH from 6.0 to 6.57, resulting in abrupt precipitation of calcite, chalcopyrite, magnetite, sphalerite and galena. Sphalerite and galena continue to precipitate down to the final analytical step. Pyrrhotite and chalcopyrite begin to precipitate at lower temperatures.

4. Discussion and Summary

The three model ore-forming processes have been analyzed to evaluate a role of boiling in mineral precipitation. Ore deposition occurs abruptly when the solution boils with the assumption of high partition of S into the vapor phase. By comparing the analytical results of the processes, it has been made clear that the role of boiling in ore formation primarily depends on the partition ratios of S between the liquid and gas phases during boiling. However, they cannot be estimated accurately by the present EOS.

Unfortunately, currently available EOS's for high P-T conditions are not sufficiently accurate for enthalpy calculations. This is the reason why we have analyzed only the processes through which temperature and pressure of the fluid are controlled externally. However, it is likely that a large amount of mineral precipitation occurs abruptly in an isenthalpic boiling process than in the present case. This is because the fluid temperature may decrease quickly during boiling by releasing evaporation enthalpy. Hence, the isenthalpic boiling may be much more effective in ore formation than the analyzed boiling process.

Acknowledgments: We thank Dr. A. Anderko for valuable discussions. Drs. J. H. Weare and N. Moller are also thanked for permitting us to access their web calculator GEOFLUIDS to check our simulation. The manuscript was greatly improved by comments made by the *Resource Geology* reviewers. This work has been supported by funds from the Ministry of Education, Culture, Sports, Science and Technology (07640641, 13640481 and 14204047).

References

Akinfiyev, N. N. (1995) A model for ore deposition from a boiling fluid: Incorporating the dielectric constant. Geochem. Intern., 32, 35–50.

Bakker, R. J. (1999) Adaptation of the Bowers and Helgeson (1983) equation of state to the H_2O-CO_2-CH_4-N_2-NaCl system. Chem. Geol., 154, 225–236.

Bottrell, S. H., Shepherd, T. J., Yardley, B. W. D. and Dubessy, J. (1988) A fluid inclusion model for the genesis of the ores of the Dolgellau Gold Belt, North Wales. Jour. Geol. Soc. London, 145, 139–145.

Bowers, T. S. (1991) The deposition of gold and other metals: Pressure-induced fluid immiscibility and associated stable isotope signatures. Geochim. Cosmochim. Acta, 55, 2417–2394.

Bowers, T. S. and Helgeson, H. C. (1983) Calculation of the thermodynamic and geochemical consequences of nonideal mixing in the system H_2O-CO_2-NaCl on phase relations in geologic systems: Equation of state for H_2O-CO_2-NaCl fluids at high pressures and temperatures. Geochim. Cosmochim. Acta, 47, 1247–1275.

Chase, M. W. Jr. (1998) NIST-JANAF Thermochemical Tables. 4th edn. American Chemical Society and American Institute of Physics. Washington, D. C., 1951p.

Cole, D. R. and Drummond, S. E. (1986) The effect of transport and boiling on Ag/Au rations in hydrothermal solutions: A preliminary assessment and possible implications for the formation of epithermal precious-metal ore deposits. Jour. Geochem. Explor., 25, 45–79.

Drummond, S. E. and Ohmoto, H. (1985) Chemical evolution and mineral deposition in boiling hydrothermal systems. Econ. Geol., 80, 126–147.

Duan, Z., Moller, N. and Weare, J. H. (1995) Equation of state for the NaCl-H_2O-CO_2 system: Prediction of phase equilibria and volumetric properties. Geochim. Cosmochim. Acta, 59, 2869–2882.

Duan, Z., Moller, N. and Weare, J. H. (1996) A general equation of state for supercritical fluid mixtures and molecular dynamics simulation of mixture PVTX properties. Geochim. Cosmochim. Acta, 60, 1209–1216.

Helgeson, H. C. and Kirkham, D. H. (1976) Theoretical predic-

tion of the thermodynamic behavior of aqueous electrolytes at high pressures and temperatures: IV. Calculation of activity coefficients, osmotic coefficients, and apparent molal and standard and relative partial molal properties to 600°C and 5 kb. Amer. Jour. Sci., 281, 1249–1516.

Holloway, J. R. (1981) Compositions and volumes of supercritical fluids in the earth's crust. *in* Hollister, L. S. and Crawford, M. L. (eds.) Short Course in Fluid Inclusions: Application to Petrology, 13–38.

Hoshino, K, Yamamoto, Y., Gu, X. P., Lee, S. Y. and Watanabe, M. (2000) Preliminary examinations of the ore-forming process by fluid mixing – a test of MIX99. Resource Geol., 50, 185–190.

Johnson, J. W., Oelkers, E. H. and Helgeson, H. C. (1992) SUPCRT92: a software package for calculating the standard molal thermodynamic properties of minerals, gases, aqueous species, and reactions from 1 to 5000 bar and 0 to 1000°C. Computer Geosci., 18, 899–947.

Kamilli, R. J. and Ohmoto, H. (1977) Paragenesis, zoning, fluid inclusion, and isotopic studies of the Finlandia vein, Colqui district, central Peru. Econ. Geol., 72, 850–982.

Lyakhov, Y. V. and Popivnyak, I. V. (1978) Physicochemical conditions of development of gold mineralization in Northern Buryatia. Intern. Geol. Rev., 20, 955–967.

Naden, J. and Shepherd, T. J. (1989) Role of methane and carbon dioxide in gold deposition. Nature, 342, 793–795.

Robert, F. and Kelly, W. C. (1987) Ore-forming fluids in Archean gold-bearing quartz veins at the Sigma mine, Abitibi greenstone belt, Quebec, Canada. Econ. Geol., 82, 1464–1482.

Wang, P. and Anderko, A. (2001) Computation of dielectric constants of solvent mixtures and electrolyte solutions. Fluid Phase Equilibria, 186, 103–122.

Wilkinson, J. J. and Johnston, J. D. (1996) Pressure fluctuations, phase separation, and gold precipitation during seismic fracture propagation. Geology, 24, 395–398.

Xie, Z. and Walther, J. V. (1995) Quartz solubilities in NaCl solutions with and without wollastonite at elevated temperatures and pressures. Geochim. Cosmochim. Acta, 57, 1947–1955.

(Editorial handling: Naoto TAKENO)